

# CrystEngComm

Accepted Manuscript



This is an *Accepted Manuscript*, which has been through the Royal Society of Chemistry peer review process and has been accepted for publication.

*Accepted Manuscripts* are published online shortly after acceptance, before technical editing, formatting and proof reading. Using this free service, authors can make their results available to the community, in citable form, before we publish the edited article. We will replace this *Accepted Manuscript* with the edited and formatted *Advance Article* as soon as it is available.

You can find more information about *Accepted Manuscripts* in the [Information for Authors](#).

Please note that technical editing may introduce minor changes to the text and/or graphics, which may alter content. The journal's standard [Terms & Conditions](#) and the [Ethical guidelines](#) still apply. In no event shall the Royal Society of Chemistry be held responsible for any errors or omissions in this *Accepted Manuscript* or any consequences arising from the use of any information it contains.



## COMMUNICATION

## Selective growth of metallic nanostructures on microstructured copper substrate in solution

Received 00th January 20xx,  
Accepted 00th January 20xx

Zhiwei He, Jianying He\*, and Zhiliang Zhang

DOI: 10.1039/x0xx00000x

www.rsc.org/

**Selective growth of metallic micro/nanostructures on desired micropatterns was achieved via a simple solution-immersion process. Interestingly, metallic micro/nanostructures directly grow only inside the hollow copper micropatterns due to the different surface properties. Furthermore, these hierarchical micro/nanostructured Cu/CuO surfaces possess superhydrophobicity, low water adhesion forces and self-cleaning properties.**

Selective growth of well-aligned nanostructures has attracted considerable attention owing to their wide range of potential applications in optoelectronic devices,<sup>1,2</sup> photovoltaic cells,<sup>3</sup> field emission devices,<sup>4</sup> gas sensors,<sup>5</sup> transistors,<sup>6</sup> and so on. Many methods, such as patterning and self-assembly growth, however, require high temperature, expensive equipment, complex multi-steps and catalysts.<sup>3,4</sup> It would be a step forward to develop a high efficient and large-scale fabrication method to achieve such selective growth of micro/nanostructures on different substrates. Recently, selective growth of ZnO nanostructures was obtained through photolithography and solution-based synthesis.<sup>3,4</sup> Schumann et al. presented catalyst-free selective growth of GaN nanowires by rf-plasma-assisted molecular beam epitaxy.<sup>2</sup> Selective growth of carbon nanotubes, as prepared by Choi et al., enabled device integration to carbon nanotube field-effect transistors.<sup>6</sup> Ordered microcontainers with CuO nanowires growing only inside were prepared by photolithography and thermal oxidation in air.<sup>7</sup>

Copper, as a well-known engineering material, is widely used in various industrial applications. In recent years, a lot of efforts have been made to fabricate hierarchical micro/nanostructured CuO, including solution-based methods,<sup>8</sup> solid-state thermal conversion of precursors,<sup>9</sup> jet nebulizer spray pyrolysis,<sup>10</sup> electrochemical methods,<sup>11-13</sup> hydrothermal synthesis,<sup>14-17</sup> thermal oxidation methods<sup>18-21</sup> and other synthetic methods.<sup>22-24</sup> Among others, the solution-immersion method is promising for high efficient and large-scale fabrication. For example, several superhydrophobic CuO flower-like micro/nanostructures were obtained by a solution-immersion process.<sup>25-28</sup> Copper hydroxide

nanotube arrays on the surface of copper substrates were facilely fabricated by immersing copper foils in an alkaline solution.<sup>29,30</sup> Similarly, copper surfaces with nanoribbon structures showed excellent superhydrophobic properties after the immersion reaction followed by the fluorination treatment.<sup>31</sup> Self-assembled polycrystalline CuO nanochains, as fabricated in aqueous medium by Gaur et al., displayed a multifunctional properties.<sup>32</sup> Chaudhary et al. synthesized CuO/Cu(OH)<sub>2</sub> hierarchical structure by a simple solution-immersion process at room temperature without using a low surface energy material.<sup>33</sup> Akhavan et al. also prepared CuO/Cu(OH)<sub>2</sub> hierarchical nanostructures as nano-photocatalysts through an *in situ* oxidation method.<sup>34</sup> Besides, Schlur et al. reported Cu(OH)<sub>2</sub> and CuO nanotube arrays in alkaline solutions on a silicon wafer instead of copper films.<sup>35</sup> Although various micro/nanostructured CuO were prepared in the alkaline solution, the selective growth on certain part of surfaces was rarely reported. In general, the metallic micropatterns could be obtained through a microfabrication process. However, this results in homogeneous surface property between the metal substrate and micropatterns, which indicates even growth of nanostructures in solution. One possible approach to different surface properties of hierarchical structure is to combine photolithography with chemically assisted ion beam etching (CAIBE). The former is used to fabricate micropatterns on the substrate, whereas the latter is to modify the surface property by etching with different gases (e.g., Ar, O<sub>2</sub>, and Cl<sub>2</sub>).

Herein, we present a new approach to control the selective growth of metallic micro/nanostructures on desired surface areas. Copper micropillars were obtained by photolithography and CAIBE, and the surface modification was achieved by changing different etching gases during a CAIBE process. As a result, the selective growth of metal based micro/nanostructures in solution become possible owing to the different surface properties between substrate and micropillars. The growth process is described in Scheme 1. To our best knowledge, this is for the first time to report selective growth of copper and silver based micro/nanostructures by a solution-immersion process.



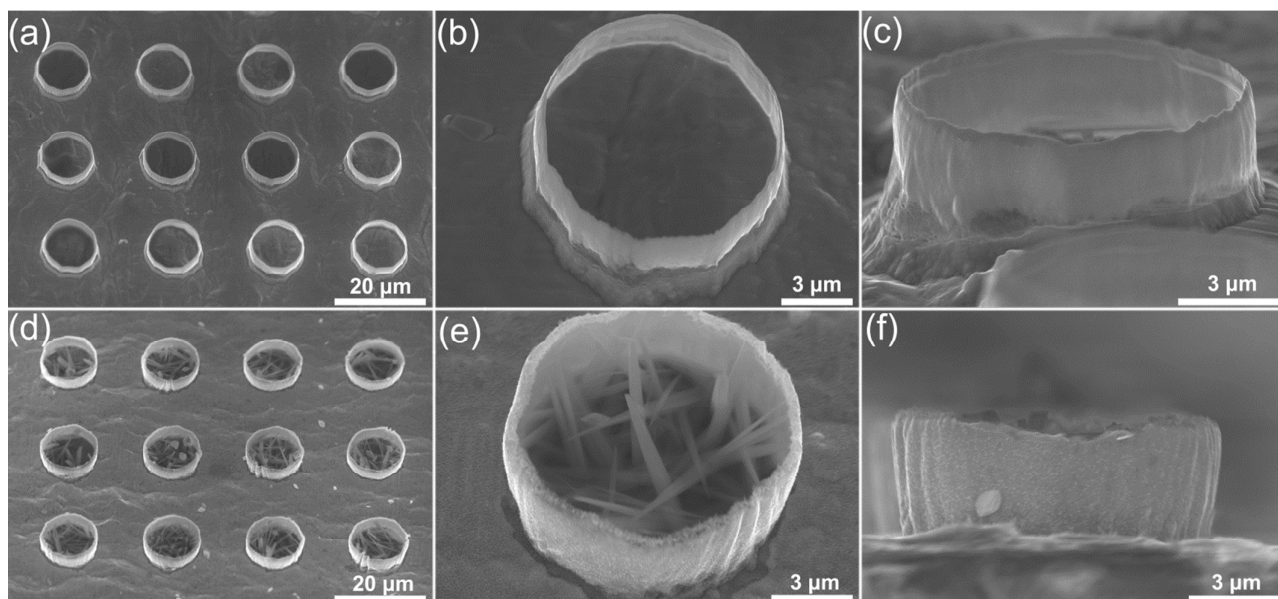


**Figure 1.** The micro- and nano- structure obtained from the process A: (a, b and c) the hollow copper micropillars obtained with the etching time by Ar and O<sub>2</sub> 30 min and 10 min, respectively; (d, e and f) nanoneedles grown inside the micropillars after 30 min solution-immersion reaction.

When the above copper micropillars are immersed in an alkaline solution, CuO nanoneedles are observed growing inside the hollow copper micropillars (Figure 1 d and e). Because the copper surface on the substrate and outside walls of hollow copper micropillars are oxidized after O<sub>2</sub> etchings, leading to delaying the formation of CuO nanoneedles in an appropriate time. But the copper surfaces inside hollow copper micropillars are protected by carbon layers and residual photoresist, and the bare copper surface inside hollow micropillars still exists after O<sub>2</sub> etchings. Besides, the growth of CuO only inside hollow micropillars confirms that bare copper surfaces inside copper micropillars have a priority for the growth of CuO nanostructures in an appropriate time (e.g., 45 min) than that of oxidized substrate surfaces. Therefore, different surface properties between inside and outside of MN1 are the critical reason that results in the growth of CuO nanoneedles only inside hollow micropillars.

Meanwhile, the wall and substrate surfaces outside the micropillars form a very thin oxidized layer (Figure 1f), in agreement with the EDS analysis. When the etching time is changed, the thickness of the walls of copper micropillars would also be changed, as shown in Figure S4. The walls of copper micropillars are wrinkled after the immersion reaction because the thin walls are formed with less copper re-deposition in 10 min during the Ar etching step. More interestingly, both nanoneedles (NN) and leaf-like nanostructures grow inside copper micropillars (Figure S4 b-d). According to the Figure S4a, leaf-like nanostructures grow over the nanoneedles (labeled as NN), similar as the growth of nanostructures on bare copper substrates (Figure S5 b-d) and other results.<sup>27, 28</sup>

In parallel, the fabrication process B revealed in Scheme 1 is investigated in order to confirm the role of CAIBE. Compared with the process A, the oxygen etching is overleapt during the process B so that the carbon layer and residual photoresist are kept to

delay the growth of CuO nanoneedles inside hollow micropillars; and they will be removed as the reaction goes. After the process B, another hierarchical micro/nanostructured Cu/CuO (MN2) is obtained, as shown in Figure 2a,b,d&e and Figure S6. The photographs of MN1 and MN2 in Figure S7 clearly display different colors, indicating different growth processes.

In the process B, 11- $\mu$ m long nanoneedles spread evenly around the hollow copper micropillars due to the uniform positive curvature surfaces of micropillars. Compared with the process A, the outside walls of hollow copper micropillars are still copper instead of CuO, whereas inside copper surfaces delay the growth of CuO by carbon layers and residual photoresist. The TEM images present that these nanoneedles taken from the original 11- $\mu$ m long nanoneedles of MN2 have CuO/CuO core-shell structures (Figure 3b), which is in agreement with the inhomogeneous element densities of oxygen and copper of the EDS images in Figure S8. It may be concluded that the formation of these CuO core-shell structures is largely due to different growth rates in different directions. The growth rate along nanoneedle is much faster than that along the radial direction, which leads to inhomogeneous element densities of oxygen and copper and the formation of core-shell structures. Moreover, many CuO nanocrystals in different size are observed in Figure 3c, and their orientations are random. In Figure 3d, multiple and discrete spots and electron diffraction rings are also found. Therefore, these nanoneedles of MN2 can be confirmed to be a polycrystalline structure from TEM observation and electron diffraction (Figure 3c&d).<sup>30, 36</sup> Compared with the case before the immersion reaction, the thickness of micropillars walls increase after oxidation, and flower-like structures are randomly formed over the micropillars. Additionally, a few nanoneedles are seen inside hollow micropillars. This is because the carbon layer and residual photoresist delayed the growth of nanoneedles inside the micropillars. More interestingly, flower-like nanostructures also

grow over the nanoneedles inside the micropillars when the immersion reaction time increased (Figure 2b&e), as well as CuO nanoflakes over hollow micropillars (Figure S4c&d).

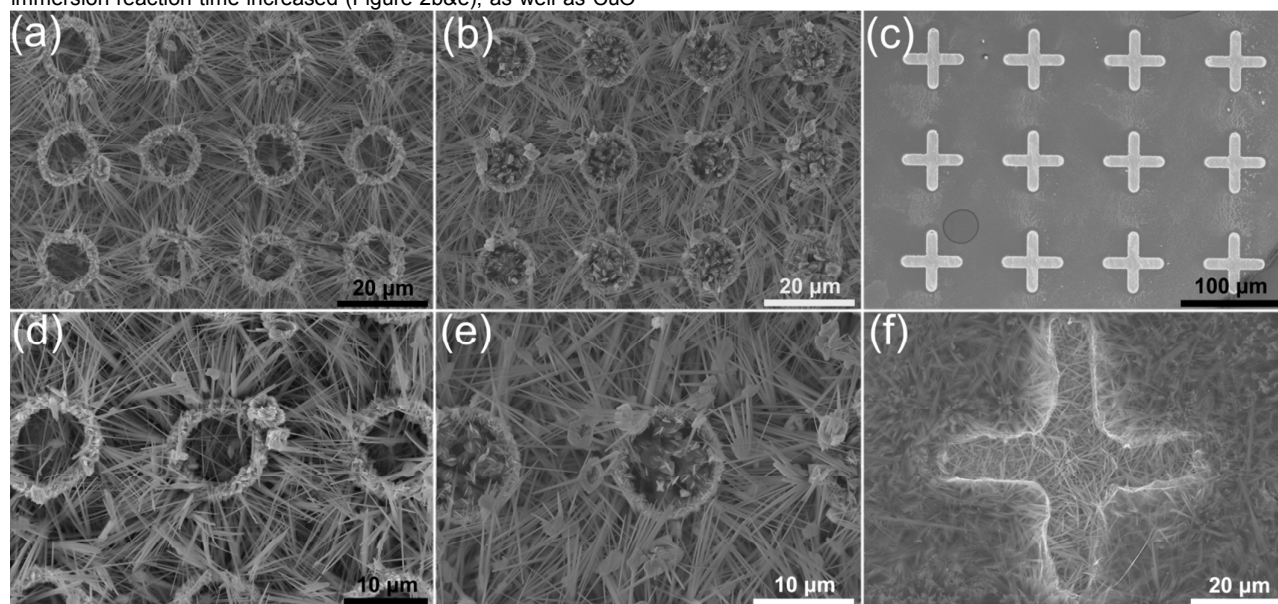


**Figure 2.** The micro/nanostructures obtained from process B with different solution-immersion reaction time: (a, d) 30 min; (b, e) 45 min; (c) cross-shaped grooves before the Ar etching and (f) nanoneedles growing with solution-immersion reaction time 45 min.

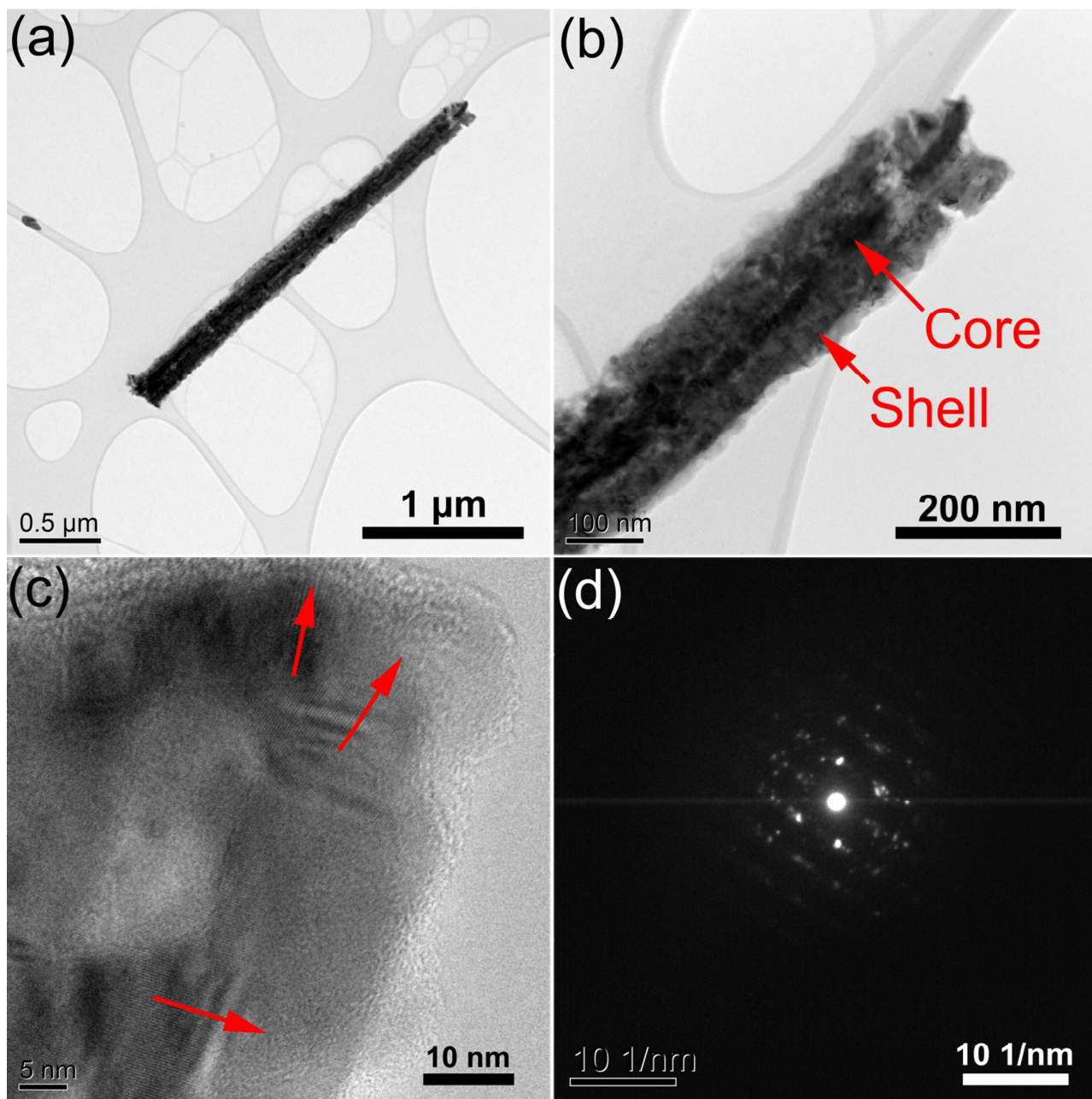


**Figure 3.** TEM images of a CuO nanoneedle of MN2: (a) and (b) core-shell structured nanoneedle in different magnification; (c) the shell morphology of highlighted area in (b), showing nanocrystalline structure; and (d) corresponding electron diffraction pattern of the shell in (c).

In the case of cross-shaped groove micropatterns on copper foil substrates, the similar growth process is found as shown in Figure 2f, and the nanostructures inside and outside the grooves exhibit different morphologies. The diameter of nanostructures inside micropatterns is smaller than that outside, similar to the delayed growth of nanostructures inside MN2. To further understand the role of CAIBE for MN1 and MN2, the bare copper foils and photoresist micropillars substrates are also investigated by the solution-immersion method and the results are shown in Figure S5 b-d and Figure S1 e-h, respectively. Compared with the bare copper after the immersion reaction, there are no microflowers over nanoneedles, indicating that the role of the

photoresist layer as well as the carbon layers is only to delay the immersion reaction. It can be concluded that the Ar etching is necessary for preparing copper micropillars, while the oxygen etching is indispensable for attaining different surface properties between the substrate and micropatterns to selective growth.

To affirm the selective growth of nanostructures inside hollow micropillars, different micropatterns of metal Ag are tested on copper substrates. In Figure 4a-d, dendritic and hexagonal micro/nanostructures are observed growing mainly inside the cross-shaped grooves where the surfaces are bare copper. The EDS images (Figure 4e&f) also demonstrate that these dendritic and hexagonal micro/nanostructures are silver. This is because

the bare copper surfaces exist on cross-shaped groove micropatterns where the replacement reaction happens as displayed in Figure 4g. Therefore, these results also demonstrate the reason why CuO nanoneedles mainly grow inside hollow copper micropillars and the growth of different silver structures is delayed in a short time because of the oxidized layer of CuO outside micropillars. Furthermore, the dendritic silver is influenced by silver ion concentration, and the growth of hexagonal structured silver is found due to a time-dependent replacement reaction of silver for copper (Figure 4b&c).<sup>37-39</sup> In this formation process, initial silver dendrites experience a morphological

evolution and convert to hexagonal nanoplates,<sup>37</sup> and then they continue to grow bigger as well as the replacement reaction proceeded as shown in Figure 4c. In the case of obtained small Cu hollow micropillars, however, air bubbles trapped inside micropillars delay the replacement reaction of Ag; while the reaction firstly happens on other surfaces because these surfaces are not fully covered by CuO. This implies that the growth of Ag nanostructures is Cu micropattern geometry and size dependent. The purpose of Ag nanostructures on Cu grooves is to demonstrate that the proposed solution-immersion method can be applied to other micropatterns with different geometries and sizes.

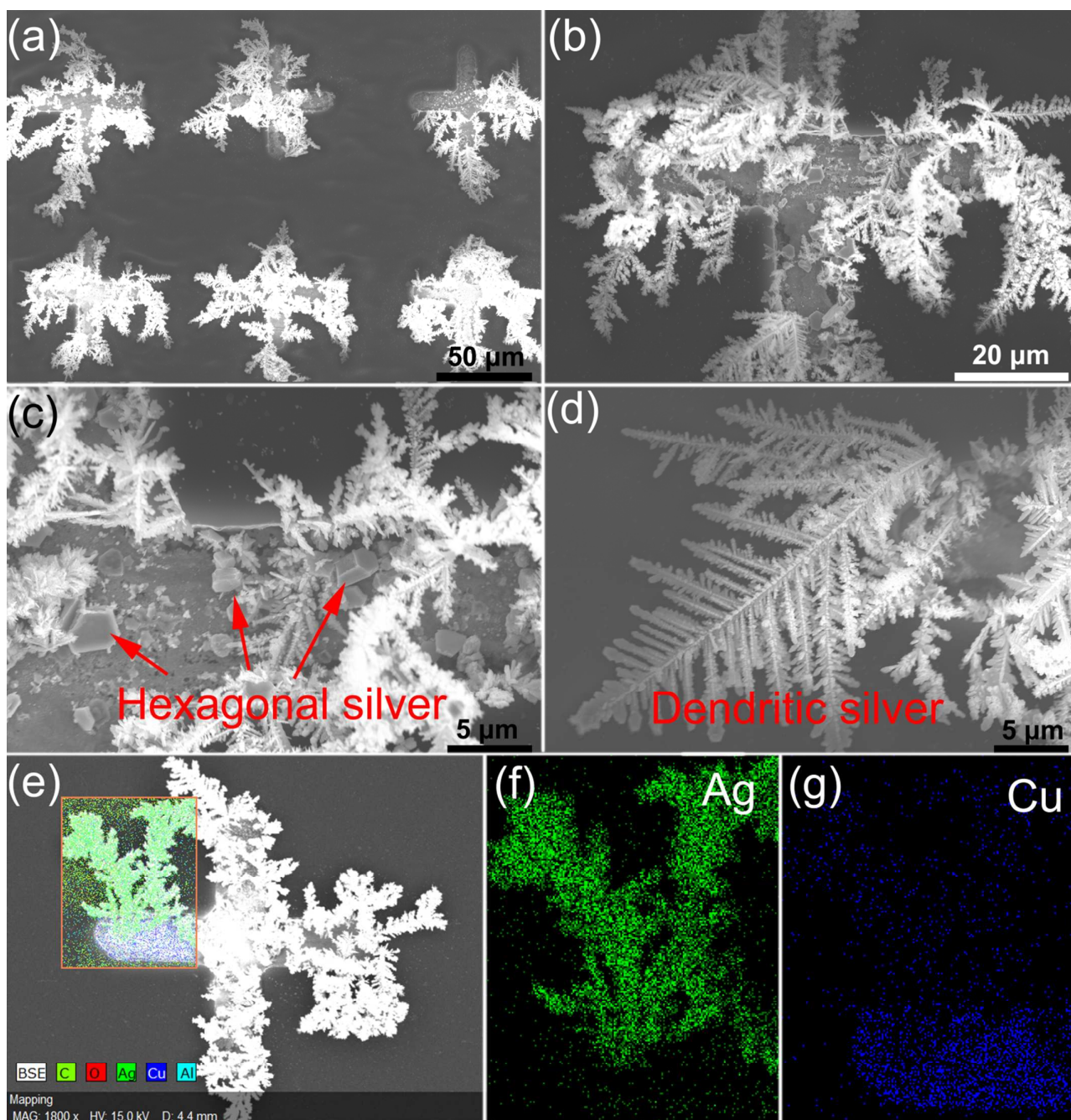


**Figure 4.** (a-d) The silver nanostructure on the copper cross-shaped groove microstructures etched by both Ar and O<sub>2</sub> for 30 min and 10 min, respectively, in process A. The subsequent solution-immersion reaction time in 0.01 M AgNO<sub>3</sub> solution was 5 min; (e-g) EDS images of the above micro/nanostructures.

Considering the difference between MN1 and MN2, the surface properties of MN1 and MN2 are examined by a low angle (3°) X-ray diffraction (XRD), as shown in Figure 5a. Both MN1 and MN2 show similar XRD patterns, but they have big differences at three peaks of 43.4°, 50.5°, and 56.2°. Surprisingly, these three peaks represent the bare copper.<sup>27, 30, 33</sup> Compared with the bare copper, MN1 lose the peak at 56.2° because of a thin oxidized

layer outside MN1, leading to the growth of nanostructures only inside hollow micropillars. As for MN2, however, the peaks at 43.4° and 56.2° are very strong because the nanostructures also grow on the substrate, resulting in the intensity increase.<sup>27, 30, 33</sup> These results further prove that the surface properties of MN1 and MN2 are different after the CAIBE process A and B.

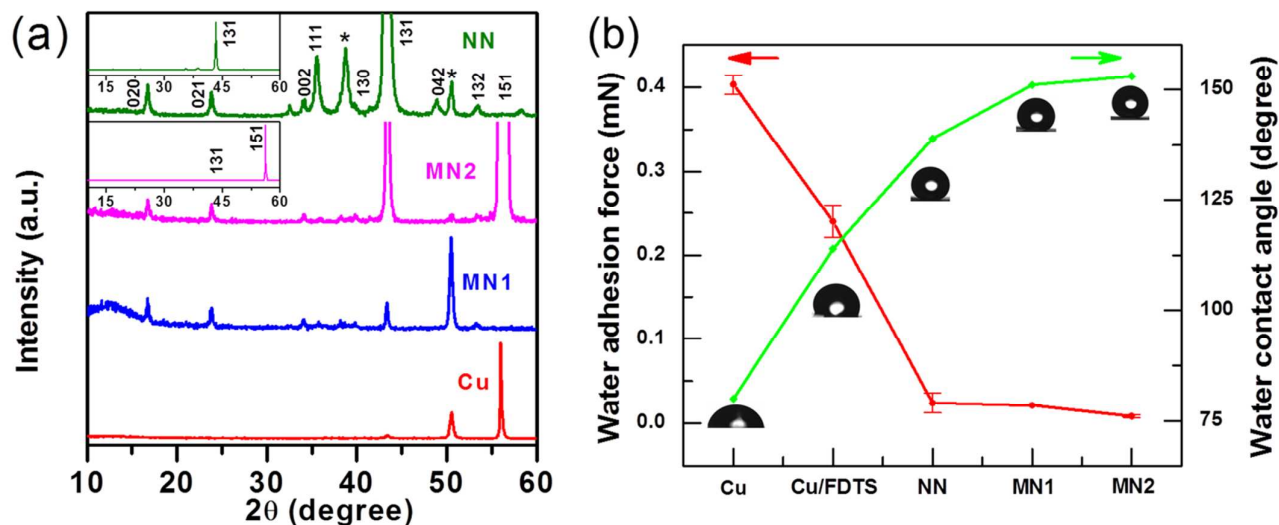


**Figure 5.** (a) The XRD patterns with an incident angle of 3° and a scan angle range of 10-60°; (b) water adhesion forces and contact angles of Cu, Cu modified with FDTS, NN, MN1 and MN2 with the modification of FDTS. NN refers to CuO nanoneedles on bare copper substrate.

In Figure 5b, the water contact angles (CAs) and water adhesion forces are displayed to verify the surface properties. The CAs of MN1 and MN2 with the modification of FDTS are 151° and 159°, respectively, while CAs of NN with the modification of FDTS is only 139°. It means that both microstructures and nanostructures are essential for preparing superhydrophobic surfaces. Moreover, the water adhesion forces for MN1 and MN2 are 14.8 and 8.33 μN, respectively, signifying their very low surface energy.<sup>40</sup> Therefore, such advantages of MN1 and MN2 offer a great potential in various applications, such as self-cleaning, anti-fouling, and anti-icing surfaces.

To observe self-cleaning properties of MN1 and MN2, an abundant amount of carbon black powder or chalk dust was dispersed on the surfaces of MN1 and MN2, and then water was slowly dripped onto these contaminated surfaces (Figure S9 a&b). The first few drops immediately rolled off from MN1 and MN2, and took away carbon black or chalk dust. Subsequently, the surfaces of MN1 and MN2 were cleaned thoroughly by enough water drops, indicating their excellent self-cleaning behaviors. Furthermore, a water jet impact test was also studied to demonstrate the stability of superhydrophobic properties of MN1 and MN2 (Figure S9c), for a high speed water jet impact might damage a coating surface and degrade its wetting properties.<sup>41, 42</sup> In Figure S9c, the water jet couldn't reflect from pure copper surface and MN1 at an angle of 45°, and spread on these surfaces. However, the water jet easily repelled off from MN2 and its superhydrophobicity is unchanged after such water jet impact test. Therefore, MN2 has

much better stability of superhydrophobicity than that of MN1, which might be due to their different micro/nanostructures and water adhesion forces.

In summary, two kinds of highly ordered micro/nanostructured Cu/CuO are facily prepared by photolithography, CAIBE, and the solution-immersion method. Selective growth of different metallic micro/nanostructures in an aqueous solution is achieved by tuning surface properties of the substrate and micropatterns. Our approach provides a practical route towards the design and development of highly controlled growth of Cu and Ag based micro/nanostructures on different copper micropatterns in solution. Furthermore, this selective growth method might also be extended for other metallic and nonmetallic materials in solution only if different surface properties could be achieved on these materials, for which we can envision its promising applications in many fields.

The authors gratefully acknowledge the financial support from Statoil ASA (Norway) through the project of nanotechnology for anti-icing application. The authors thank NTNU NanoLab for support, in particular Espen Rogstad for a fruitful discussion of CAIBE.

## Notes and references

NTNU Nanomechanical Lab  
Department of Structural Engineering

Norwegian University of Science and Technology (NTNU)  
Trondheim, 7491, Norway  
E-mail: [jianying.he@ntnu.no](mailto:jianying.he@ntnu.no)  
Homepage: <http://www.ntnu.edu/nml>

1. Y. J. Hong, S. J. An, H. S. Jung, C. H. Lee and G. C. Yi, *Adv. Mater.*, 2007, **19**, 4416-4419.
2. T. Schumann, T. Gotschke, F. Limbach, T. Stoica and R. Calarco, *Nanotechnology*, 2011, **22**, 095603.
3. C. H. Wang, A. S. W. Wong and G. W. Ho, *Langmuir*, 2007, **23**, 11960-11963.
4. Q. Ahsanulhaq, J.-H. Kim and Y.-B. Hahn, *Nanotechnology*, 2007, **18**, 485307.
5. X. Wang, F. Sun, Y. Huang, Y. Duan and Z. Yin, *Chem. Commun.*, 2015, **51**, 3117-3120.
6. W. B. Choi, B. H. Cheong, J. J. Kim, J. Chu and E. Bae, *Adv. Funct. Mater.*, 2003, **13**, 80-84.
7. P. Shao, S. Deng, J. Chen and N. Xu, *Nanoscale Res. Lett.*, 2011, **6**, 1-4.
8. J. Y. Xiang, J. P. Tu, L. Zhang, Y. Zhou, X. L. Wang and S. J. Shi, *J. Power Sources*, 2010, **195**, 313-319.
9. Y. Zhao, J. Zhao, Y. Li, D. Ma, S. Hou, L. Li, X. Hao and Z. Wang, *Nanotechnology*, 2011, **22**, 115604.
10. S. S. Latthe, P. Sudhagar, C. Ravidhas, A. Jennifer Christy, D. David Kirubakaran, R. Venkatesh, A. Devadoss, C. Terashima, K. Nakata and A. Fujishima, *CrystEngComm*, 2015, **17**, 2624-2628.
11. M. Xu, F. Wang, B. Ding, X. Song and J. Fang, *RSC Adv.*, 2012, **2**, 2240-2243.
12. F. Xiao, S. Yuan, B. Liang, G. Li, S. O. Pehkonen and T. Zhang, *J. Mater. Chem. A*, 2015, **3**, 4374-4388.
13. W. Liang, L. Zhu, W. Li and H. Liu, *RSC Adv.*, 2015, **5**, 38100-38110.
14. D. P. Volanti, M. O. Orlandi, J. Andres and E. Longo, *CrystEngComm*, 2010, **12**, 1696-1699.
15. C. Wang, Y. Ye, B. Tao and B. Geng, *CrystEngComm*, 2012, **14**, 3677-3683.
16. X. Liu, J. Zhang, Y. Kang, S. Wu and S. Wang, *CrystEngComm*, 2012, **14**, 620-625.
17. Y. Zhao, H. Shi, M. Chen and F. Teng, *CrystEngComm*, 2014, **16**, 2417-2423.
18. X. Jiang, T. Herricks and Y. Xia, *Nano Lett.*, 2002, **2**, 1333-1338.
19. F. Gao, H. Pang, S. Xu and Q. Lu, *Chem. Commun.*, 2009, 3571-3573.
20. A. Li, H. Song, J. Zhou, X. Chen and S. Liu, *CrystEngComm*, 2013, **15**, 8559-8564.
21. F. Wu, Y. Myung and P. Banerjee, *CrystEngComm*, 2014, **16**, 3264-3267.
22. Q. Zhang, K. Zhang, D. Xu, G. Yang, H. Huang, F. Nie, C. Liu and S. Yang, *Prog. Mater. Sci.*, 2014, **60**, 208-337.
23. G. Qiu, S. Dharmarathna, Y. Zhang, N. Opembe, H. Huang and S. L. Suib, *J. Phys. Chem. C*, 2011, **116**, 468-477.
24. Y. Na, S. W. Lee, N. Roy, D. Pradhan and Y. Sohn, *CrystEngComm*, 2014, **16**, 8546-8554.
25. J. Liu, X. Huang, Y. Li, K. M. Sulieman, X. He and F. Sun, *J. Mater. Chem.*, 2006, **16**, 4427-4434.
26. Q. Pan, J. Liu and Q. Zhu, *ACS Appl. Mater. Interfaces*, 2010, **2**, 2026-2030.
27. X. Chen, L. Kong, D. Dong, G. Yang, L. Yu, J. Chen and P. Zhang, *J. Phys. Chem. C*, 2009, **113**, 5396-5401.
28. J. Li, X. Liu, Y. Ye, H. Zhou and J. Chen, *J. Phys. Chem. C*, 2011, **115**, 4726-4729.
29. X. Chen, L. Kong, D. Dong, G. Yang, L. Yu, J. Chen and P. Zhang, *Appl. Surf. Sci.*, 2009, **255**, 4015-4019.
30. W. Zhang, X. Wen, S. Yang, Y. Berta and Z. L. Wang, *Adv. Mater.*, 2003, **15**, 822-825.
31. J. Feng, Z. Qin and S. Yao, *Langmuir*, 2012, **28**, 6067-6075.
32. U. K. Gaur, A. Kumar and G. D. Varma, *CrystEngComm*, 2014, **16**, 3005-3014.
33. A. Chaudhary and H. C. Barshilia, *J. Phys. Chem. C*, 2011, **115**, 18213-18220.
34. O. Akhavan, R. Azimirad, S. Safa and E. Hasani, *J. Mater. Chem.*, 2011, **21**, 9634-9640.
35. L. Schlur, K. Bonnot and D. Spitzer, *RSC Adv.*, 2015, **5**, 6061-6070.
36. C. Deng, H. Hu, X. Ge, C. Han, D. Zhao and G. Shao, *Ultrason. Sonochem.*, 2011, **18**, 932-937.
37. J. Fang, H. You, P. Kong, Y. Yi, X. Song and B. Ding, *Cryst. Growth Des.*, 2007, **7**, 864-867.
38. Z.-W. He, Q.-F. Lü and J.-Y. Zhang, *ACS Appl. Mater. Interfaces*, 2012, **4**, 369-374.
39. Y. Xiong, I. Washio, J. Chen, M. Sadilek and Y. Xia, *Angew. Chem. Int. Ed.*, 2007, **46**, 4917-4921.
40. S. Feng, S. Wang, L. Gao, G. Li, Y. Hou and Y. Zheng, *Angew. Chem. Int. Ed.*, 2014, **53**, 6163-6167.
41. H. Yoon, H. Kim, S. S. Latthe, M.-w. Kim, S. Al-Deyab and S. S. Yoon, *J. Mater. Chem. A*, 2015, **3**, 11403-11410.
42. S. S. Latthe, C. Terashima, K. Nakata, M. Sakai and A. Fujishima, *J. Mater. Chem. A*, 2014, **2**, 5548-5553.

## A table of contents

Two kinds of micro/nanostructured superhydrophobic CuO surfaces were achieved by solution-immersion method.

